CIVIL ENGINEERING JOURNAL

Article no. 2

THE CIVIL ENGINEERING JOURNAL 1-2025

AN ANALYTICAL INVESTIGATION ON NONLINEAR FREE VIBRATIONS OF BEAM WITH A FATIGUE-CRACK

Qiang Li [1,2] and Qingze Tian [1,2]

1. *School of Intelligent Manufacturing, Taizhou University, Taizhou 318000, China; liqiang1988@tzc.edu.cn*
2. *Institute of Robotics and Intelligent Systems, Taizhou University, Taizhou 318000, China; tianqingze92@gmail.com*

Received: *22.06.2024*

Received in revised form: *09.01.2025*

Accepted: *11.03.2025*

ABSTRACT

This study examines the nonlinear free vibration behavior of beams affected by a fatigue crack. Initially, transverse vibrations of a cantilevered beam are demonstrated as a single-degree-of-freedom system with equivalent mass and stiffness in the first mode. Subsequently, a novel bilinear stiffness model for beams with breathing cracks is introduced. Utilizing this model, the governing differential formula is formulated analytically using the Lindest-Poincaré perturbation method. The results indicate that the response derived through the perturbation method comprises 2 distinct components. With stiffness equal to the mean of the crack's completely open and fully closed states, the first component depicts the system's reaction. The additional correction terms, supplementing the initial response, account for variations in stiffness resulting from crack opening and closing dynamics. These corrections elucidate the impact of changing equivalent stiffness on the system's response due to crack dynamics. Indeed, the correction terms encompass higher harmonic components that emerge in the response, stemming from the nonlinear behavior of the structure. These additional terms capture the intricate interplay between crack dynamics and system response, providing a comprehensive understanding of the system's nonlinear characteristics.

KEYWORDS

Nonlinear vibration, Fatigue-crack, Bilinear stiffness, Natural frequency, Analytical method

INTRODUCTION

Fatigue cracks frequently manifest in structural components subjected to repetitive loads, posing a risk of failure if left undetected. Studies indicate distinguishable dynamic responses between defective and healthy structures, offering a potential avenue for detecting defects such as crack depth and location by quantifying these differences based on a model of the defective structure [1-3]. The majority of research in this area relies on linear models, where structural cracks are typically represented as continuously open grooves. In these models, alterations in natural frequencies and vibration mode shapes serve as primary indicators for detecting defects within the structure [4-7].

Dynamic analysis of cracked configurations holds promise as a valuable indicator for diagnosing faults. By examining the nonlinear behavior of vibrations, such as changes in frequency, amplitude, or mode shapes, engineers can detect and characterize structural defects, including

cracks [8-10]. Vibration analysis offers advantages over traditional linear approaches, as it can reveal subtle changes in structural behavior that may indicate the presence of defects even in their early stages [11-13]. Therefore, leveraging vibration analysis can enhance the accuracy and effectiveness of defect diagnosis in structures. In the context of crack modeling, numerous researchers have explored various models. For example, Rezaee and Maleki [14] examined the nonlinear behavior of a beam containing both open and closed cracks within its primary vibration mode. To this end, by some realistic presumptions, novel functions for displacement and stress fields are recommended. Peng et al. [15] performed an exploration focusing on the nonlinear characteristics of cracks through employing nonlinear output frequency response functions. Their analysis discerned that these graphs, elicited by system stimulation at optimal frequencies, exhibit pronounced sensitivity towards the detection of fatigue-induced cracks. Kharazan et al. [16] explore the nonlinear dynamics behavior of a cantilever beam affected by multiple breathing cracks. Their approach involves calculating the stiffness of a multi-cracked beam by introducing the concept of effective length to accommodate local stiffness reduction near cracks. Their research reveals that beams with a greater number of cracks or deeper cracks demonstrate significant softening behavior. Consequently, this softening behavior results in more prominent jumps in the system's response. Ma et al. [17] introduced a loose coupling analysis tactic for conducting vibration fatigue analysis on a simply supported beam subjected to typical harmonic excitation. The method assumes that the crack does not propagate during each vibration cycle but rather grows at the end of each cycle. This approach allows for a detailed investigation of the fatigue behavior of the structure under cyclic loading conditions, considering the dynamic effects of crack propagation on the overall system response. Zao et al. [18] conducted a nonlinear forced vibration analysis of an Euler-Bernoulli beam with multi-cracked while incorporating damping effects. Their study aimed to investigate the dynamics of a curved beam afflicted with multiple cracks under external excitation, considering nonlinearities and damping influences. Gaderi et al. [19] explored the dynamic and stability characteristics of cracked columns under axial load. Their study investigated the dynamic response and buckling of cracked columns under axial load. They researched the vibration and stability characteristics of columns with cracks to offer information on the behavior that may be exhibited by such columns, including possible modes of failure, which is vital in ensuring safety and reliability in structural systems for engineering applications. Long et al. [20] were motivated by the necessity for condition monitoring and fault diagnostics of beams employed in vibrating screens within the mining industry. In response to this challenge, they sought to establish a dependable model-based approach. Their focus centered on devising a novel stiffness matrix for a finite element to accurately simulate a beam affected by a breathing crack. Aggumus et al. [21] investigated the effects of cracks in the columns of a single-degree-of-freedom steel structure scheme on system responses, focusing on the reduction in the equivalent spring coefficient. Hai and Nam [22] presented a simplified pattern of a cracked beam using a single-degree-of-freedom system. The equivalence between the beam and SDOF models ensures that they share the same fundamental natural frequency and exhibit similar frequency response functions. Kharazan et al. [16] explored the nonlinear vibration behavior of a cantilever beam with multiple breathing cracks. To achieve this, they calculated the stiffness of the multi-cracked beam by introducing an effective length that accounts for the local stiffness reduction near the cracks. Additionally, Liu et al. [23] proposed a tactic for determining breathing fatigue cracks in compressor blades by leveraging the nonlinear characteristics induced by the cracks.

Although many works recognize the presence of harmonic components in the dynamic response of faulty structures and their sensitivity to crack parameters, the time evolution of system parameters and the analytical explanation of such behavior is a challenging task. Therefore, most of the studies in this field are performed with the help of numerical or finite element methods. Yet their inherent numerical nature and computationally lengthy procedures make such approaches practically inapplicable for definition of dynamic fault indicators within the frames of vibration-based troubleshooting techniques. Recent research has indeed been conducted into the nonlinear dynamics of cracked structures through various methods of modeling. SDOF models have widely been used to simplify the system, while a bilinear stiffness model effectively realizes the dynamic

behavior of the crack opening and closing. Perturbation methods, among which the Lindest-Poincaré method is very outstanding, have emerged as powerful tools for studying nonlinear characteristics. However, substantial challenges arise. Most of the existing models fall short of providing an accurate description of the detailed impact of crack dynamics on the harmonic response of the system. Moreover, comprehensive studies that establish analytical relations between crack parameters depth and position-with the ensuing nonlinear behavior are scant. These lacunae indicate the need for more robust models and analytical approaches to enhance the understanding of cracked beam dynamics.

This work seeks to relate the harmonic components present in the frequency spectrum of vibration responses of a cracked beam to both crack parameters and system characteristics analytically, with the help of the Lindest-Poincaré perturbation method. The transverse vibrations of a single-crack beam with open and closed fatigue cracks are modeled as a single-degree-of-freedom oscillator with bilinear stiffness. Accordingly, a new model for bilinear stiffness is presented, and by performing the mathematical operations and using the Lindest-Poincaré method, the governing differential formula is brought to a standard analyzable form. Then, employing the Lindest-Poincaré method, the system response is obtained, and the results are verified using numerical methods. This novelty develops the representative modeling of structural beams with cracks better and allows for better condition monitoring and fault diagnosis of vibrating screens in mining operations.

SDOF MODEL OF A CRACKED BEAM

In this study, an equivalent mass and stiffness SDOF system represents the free vibrations of a cantilever beam displaying a transverse fatigue fracture in its initial vibration mode (Figure 1). This modeling approach is grounded in equating the kinetic and potential energies of the cracked beam with those of the equivalent degree of freedom framework.

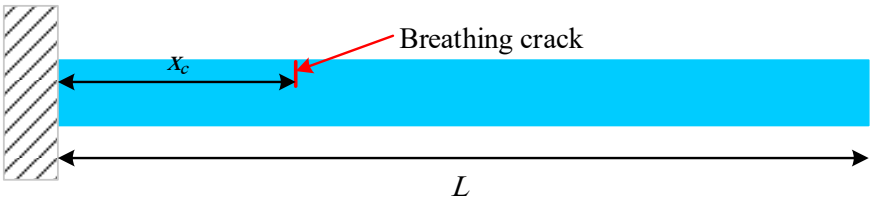

(a)

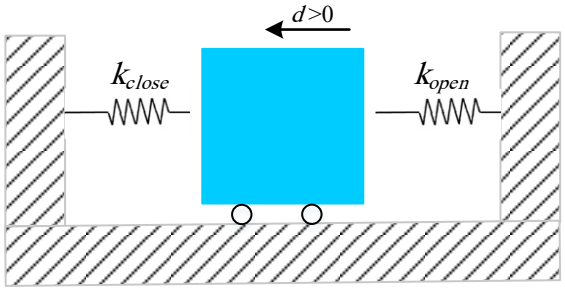

(b)

Fig. 1 - (a) Cantilever beam crack in and (b) the corresponding SDOF model

The studies conducted on fatigue crack behavior display that the non-linear load-displacement relationship of the cracked structure can be considered almost as a bilinear relationship [24] (Figure 2). As a result, when the beam vibrates, by changing the state of the crack between completely open and completely closed states, the equivalent stiffness changes between the equivalent stiffness values corresponding to these states.

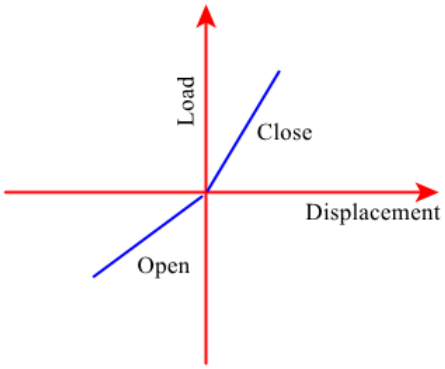

Fig. 2 - Fatigue crack in the fractured beam's bilinear load-displacement diagram.

The bilinear stiffness model, which consists of the combination of 2 lines with different slopes, is a function of the oscillation amplitude and is expressed as follows:

$$k(d) = \begin{cases} k_{close} & d > 0 \\ k_{open} & d < 0 \end{cases} \quad (1)$$

Where the comparable stiffnesses in the completely open and fully closed crack states are represented, respectively, by the variables k_{open} and k_{close}. The equivalent stiffness of an intact beam is derived according to:

$$k_c = \frac{1}{C_c} = \int_0^L EI\varphi''^2(x)dx \quad (2)$$

In this equation, C_c stands for the flexibility of a healthy structure, E is elastic modulus, I stands for the cross-section moment and L is the length. It is supposed that by applying suitable initial conditions, the beam vibrates in the first mode, so the mode shape of the first vibration of the beam is monotonous. Mukhopadhyay [25] has proposed the following approximate relationship to calculate the form of the first vibration mode of a cantilever beam:

$$\psi(x) = 1 - cos\left(\frac{\pi}{2}\frac{x}{L}\right) \quad (3)$$

In most of the research in this field, the above relationship has been used to derive the equivalent mass and stiffness of the system. In this research, to increase the accuracy, the shape of vibration modes of the Euler-Bernoulli beam, which are obtained from the analytical solution of the equations of motion below, have been used:

$$\varphi(x) = cos\,\beta\,x - cosh\,\beta\,x - \frac{(sin\,\beta\,x - sinh\,\beta\,x)(cos\,\beta\,L + cosh\,\beta\,L)}{(sin\,\beta\,L + sinh\,\beta\,L)} \quad (4)$$

In the above equation, the shape of the first vibration mode is obtained $\lambda L = 1.875$. Figure 3 shows the disparity between the analytical mode shape used in the current research and the approximate mode shape proposed in Ref. [25].

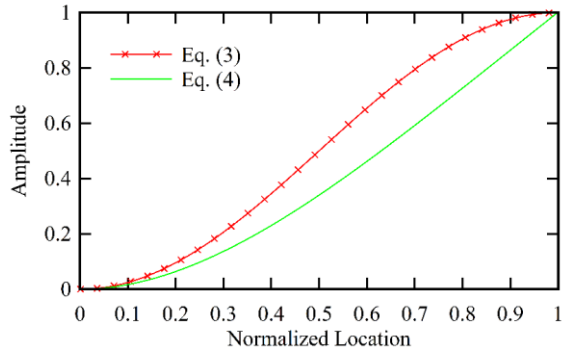

Fig. 3 - The initial mode form of a clamped-free beam, derived from the approximation function suggested in Ref. [19] *and the analytical resolution of the Euler-Bernoulli beam motion equations*

The equivalent stiffness with a completely open crack is obtained from the following relationship:

$$k_\circ = \frac{1}{C_\circ} \tag{5}$$

When the existence of fractures causes a change in the beam's flexibility (ΔC), expressed as $C_\circ = \Delta C + C$. Dimarogonas et al. [26] have presented the following relationship to determine the change in the flexibility of a cantilever beam owing to the presence of cracks deep and at a distance from the free end of the beam:

$$\Delta C = w\frac{\partial^2}{\partial {P_i}^2}\int_0^a Jda = \frac{72l_c^2\pi(1-\nu^2)}{Ewb^4}\phi \tag{6}$$

In which, *b* and *w* denote the height and width, *J* remains the strain energy release rate and *v* is Poisson's ratio, and ϕ is obtained from the following relationship:

$$\begin{aligned}\phi = \ & 19.70\frac{a^{10}}{b^8} - 40.64\frac{a^9}{b^7} + 47.45\frac{a^8}{b^6} - 32.78\frac{a^7}{b^5} + 20.89\frac{a^6}{b^4} - 9.68\frac{a^5}{b^3} \\ & +4.45\frac{a^4}{b^2} - 1.06\frac{a^3}{b} + 0.67a^2\end{aligned} \tag{7}$$

The equivalent mass of the beam is obtained as:

$$m = \int_0^L \varphi^2(x)m(x)dx \tag{8}$$

In which *m*(*x*) stands the unit mass. According to the above assumptions, the governing differential equation of the equivalent system is obtained below:

$$m\ddot{x} + k(x)x = 0 \tag{9}$$

Where *x* displays the displacement of the beam and relates to the displacement of the beam's free end.

PRESENTING A NEW MODEL FOR BILINEAR STIFFNESS OF THE CRACKED BEAM

It has been shown that if the differential equation governing a nonlinear dynamic system can be expressed in the form of Eq. (10), its answer can be obtained using the Lindest-Poincaré method, which is one of the perturbation methods [27].

$$\ddot{x} + \omega_o^2 x = \varepsilon f(x,t) \quad (10)$$

Where ε is regarded as a tiny dimensionless factor and ω_0 remains the associated linear beam's inherent frequency.

Equation 1 displays that the equivalent stiffness is a function of the oscillation amplitude. By considering the bilinear function provided for $k(d)$, the bilinear stiffness of the cracked beam is stated below:

$$\begin{cases} k_{close} = k(1+\varepsilon) \\ k_{open} = k(1-\varepsilon) \end{cases} \quad (11)$$

k displays the comparable average stiffness in the crack's completely open and fully closed states:

$$k = \frac{1}{2}\left(k_{open} + k_{close}\right) \quad (12)$$

And ε is a dimensionless and small parameter defined as follows:

$$\varepsilon = -\frac{k_{open} - k_{close}}{k_{open} + k_{close}} \quad (13)$$

Drawing from Equations 11 to 13 the subsequent novel model for the bilinear stiffness of the fractured beam is introduced:

$$k(x) = kx + \varepsilon k|x| \quad (14)$$

By substituting Equation 14 into Equation 9, the following is obtained:

$$m\ddot{x} + kx = -\varepsilon k|x| \quad (15)$$

By dividing both sides of Equation 15 on *m*, the governing differential equation is expressed in the following final form:

$$\ddot{x} + \omega_0^2 x = -\varepsilon\omega_0^2|x| \quad (16)$$

Where:

$$\omega_0 = \sqrt{\frac{k}{m}} \quad (17)$$

By comparing Equations 10 and 16, it can be seen that by presenting a new model for bilinear stiffness of the cracked beam model, the governing differential equation can be written in an analyzable form by the perturbation method. In addition, in this model, unlike time-varying stiffness models, the equivalent stiffness is a function of the oscillation amplitude, which has led to the formation of a non-linear differential equation. Certainly, such a model leads to a better understanding of the non-linear behavior of fatigue cracks compared to time-varying stiffness models.

APPLICATION OF THE LINDEST-POINCARÉ METHOD

In the current research, the Lindest-Poincaré method was used to obtain the system response [27]. Based on this, the response of the system and its frequency are considered as the following series:

$$x = x_0 + \varepsilon x_1 + \varepsilon^2 x_2 + .. \quad (18)$$

$$\omega = \omega_0 + \varepsilon\omega_1 + \varepsilon^2\omega_2 + \ldots \quad (19)$$

According to $\tau = \omega t$, the derivatives of *x* in terms of time can be expressed in terms of the new variable as:

$$\frac{dx}{dt} = \omega\frac{dx}{d\tau} = (\omega_0 + \varepsilon\omega_1 + \varepsilon^2\omega_2 + \ldots)\frac{d}{d\tau}(x_0 + \varepsilon x_1 + \varepsilon^2 x_2 + \ldots) \quad (20)$$

$$\frac{d^2x}{dt^2} = \omega^2 \frac{d^2x}{d\tau^2} = (\omega_0 + \varepsilon\omega_1 + \varepsilon^2\omega_2 + \ldots)^2 \frac{d^2}{d\tau^2}(x_0 + \varepsilon x_1 + \varepsilon^2 x_2 + \ldots) \quad (21)$$

By substituting Equations 18 to 21 in Equation 16, the following is obtained:

$$\begin{aligned}&(\omega_0 + \varepsilon\omega_1 + \varepsilon^2\omega_2 + \ldots)^2 \frac{d^2}{d\tau^2}(x_0 + \varepsilon x_1 + \varepsilon^2 x_2 + \ldots) \\ &+\omega_0^2(x_0 + \varepsilon x_1 + \varepsilon^2 x_2 + \ldots) + \varepsilon\omega_0^2|x_0 + \varepsilon x_1 + \varepsilon^2 x_2 + \ldots| = 0\end{aligned} \quad (22)$$

By arranging the above relationship in terms of increasing powers of ε, 3 differential equations are obtained as follows:

$$\varepsilon^0: \quad \omega_0^2\left(\frac{d^2x_0}{d\tau^2} + x_0\right) = 0 \quad (23)$$

$$\varepsilon^1: \quad \omega_0^2\left(\frac{d^2x_1}{d\tau^2} + x_1\right) = -2\omega_0\omega_1\frac{d^2x_0}{d\tau^2} - \omega_0^2|x_0| \quad (24)$$

$$\begin{aligned}&\varepsilon^2: \quad \omega_0^2\left(\frac{d^2x_2}{d\tau^2} + x_2\right) = \\ &-2\omega_0\omega_1\frac{d^2x_1}{d\tau^2} - (\omega_1^2 + 2\omega_0\omega_2)\frac{d^2x_0}{d\tau^2} - \omega_0^2\frac{|x_0 + \varepsilon x_1|}{x_0 + \varepsilon x_1}x_1\end{aligned} \quad (25)$$

Equation 23 is a homogeneous differential equation whose solution yields the answer of the beam with the average equivalent stiffness in both the completely closed and open states of the fracture. This system, which is called the corresponding linear system, includes the main part of the answer. Equations 24 and 25 may be solved to determine the consequences of the crack's opening and closure on the system's reaction, which is produced by a change in equivalent stiffness. In this research, the second method is used. Thus, assuming the initial conditions of net displacement, the main part of the answer is obtained from the solution of the differential Equation 23 as follows:

$$x_0 = A\cos\tau \quad (26)$$

Where in:

$$A = A_0 + \varepsilon A_1 + \varepsilon^2 A_2 \quad (27)$$

In which, A_0 is the initial displacement of the beam and A_1 and A_2 are determined in such a way that the initial conditions of the first and second-order correction sentences become zero. To remove only the secular term of Eq. (24), the following is obtained:

$$-2\omega_0\omega_1\frac{d^2x_0}{d\tau^2} = 0 \quad (28)$$

In which $\omega_1 = 0$. By removing the secular term from Equation 24 and inserting the result obtained in Eq. (26) into it, this equation is expressed as:

$$\frac{d^2x_1}{d\tau^2} + x_1 = -A|\cos\tau| \quad (29)$$

$|\cos\tau|$ is an even periodic function whose Fourier expansion is obtained as follows:

$$g(\tau) = \frac{2}{\pi} + \sum_{n=1}^{\infty}\frac{4}{\pi}\left\{\frac{1}{(1-4n^2)}(-1)^n\right\}\cos 2n\tau \quad (30)$$

Substituting Equation 30 in Equation 29, the following is obtained:

$$\frac{d^2x_1}{d\tau^2} + x_1 = -Ag(\tau) = -A\left\{\frac{2}{\pi} + \sum_{n=1}^{\infty\Sigma}\frac{4}{\pi}\left\{\frac{1}{(1-4n^2)}(-1)^n\right\}cos\,2\,n\tau\right\} \quad (31)$$

As can be seen, the right side of Equation 31 consists of a constant value and a set of harmonic terms. By solving the differential equation, the private answer is obtained as follows:

$$x_1 = -A\left\{\frac{2}{\pi} + \sum_{n=1}^{\infty}\frac{4}{\pi}\left\{\frac{1}{(1-4n^2)^2}(-1)^n\right\}cos\,2\,n\tau\right\} \quad (32)$$

In Equation 25, the expression $\left(\frac{|x_0+\varepsilon x_1|}{x_0+\varepsilon x_1}\right)x_1$ can be written as follows using Fourier expansion:

$$f(\tau) = b_0 + \sum_{m=1}^{\infty} b_m\,cos\,m\,\tau \quad (33)$$

Where the Fourier expansion coefficients are obtained as follows:

$$b_0 = \frac{1}{\pi}\left\{\int_0^z \bar{x}_1 d\tau - \int_z^{\pi}\bar{x}_1 d\tau\right\} \quad (34)$$

$$b_m = \frac{2}{\pi}\left\{\int_0^z \bar{x}_1\,cos\,m\,\tau\;d\tau - \int_z^{\pi}\bar{x}_1\,cos\,m\,\tau\;d\tau\right\},\; m = 1,2,.. \quad (35)$$

In which *z* is the place where the sign of the function $(x_0 + \varepsilon\; x_1)$ changes and the average value of $\bar{x}_1$ obtained in Equation 32. By calculating the above integrals, the Fourier expansion coefficients of Equation 33 are obtained as follows:

$$b_0 = \left(\frac{\bar{b}_1}{\pi}\right)(2z - \pi) \quad (36)$$

And:

$$b_m = \left(\frac{4\bar{b}_1}{m\pi}\right)sin\,m\,z\;, \quad m = 1,2,\ldots \quad (37)$$

By placing the Fourier expansion provided for the expression $\left(\frac{|x_0+\varepsilon x_1|}{x_0+\varepsilon x_1}\right)x_1$ in Equation 25, it can be seen that the first term of this expansion is a secular term, which requires the following relationship to be removed:

$$-2\omega_0\omega_2(-A\,cos\,\tau) - \omega_0^2(b_m\,cos\,m\,\tau)|_{m=1} = 0 \quad (38)$$

So

$$\omega_2 = \frac{\omega_0 b_1}{2\;A} \quad (39)$$

By removing the secular term from Equation 25 and solving this differential equation, the private answer is obtained as follows:

$$x_2 = b_0 + \sum_{m=2}^{\infty}\left(\frac{b_m}{1-m^2}\right)cos\,m\,\tau \quad (40)$$

in which b_0 is b_m obtained from Equations 36 and 37 respectively. Finally, the response of the beam is achieved as follows:

$$x(\tau) = x_0(\tau) + \varepsilon x_1(\tau) + \varepsilon^2 x_2(\tau) \quad (41)$$

where:

$$\tau = \omega\ t \quad (42)$$

$$\omega = \omega_0 + \varepsilon^2\omega_2 \quad (43)$$

Case Study Analysis and Discussion

The geometric dimensions and mechanical characteristics of the steel beam with a crack are investigated as follows: beam length L=500 mm, beam cross section A=4×6.5 mm^2, elastic modulus E=206 GPa, and density is ρ=7850 kg/m^3. Moreover, the relative position of the fracture is indicated by $\beta=x_c/L$, and its relative depth is shown by $\alpha=a/h$, which is the ratio of the crack's depth to the beam's thickness. The initial conditions are the same in all the cases that will be examined.

To verify the proposed model, the results from Ref. [28] are utilized. Specifically, a single beam with a length of 500 units and a cross-sectional area of 29×20 units is considered. The elastic modulus and density are assumed to be the same as previously described. Table 1 presents a comparison of the first natural frequency for varying crack depths. The results demonstrate a strong agreement between the findings of the present study and those of Ref. [28], with errors ranging from 1.06% to 3.25%. However, the natural frequencies predicted by the present study are consistently higher than those in Ref. [28], attributed to the increased equivalent stiffness in the opening-and-closing crack model.

Tab. 1 - Natural frequencies (Hz) of the cracked beam

Method	Crack depth (mm)				
	4	8	12	16	20
Present work	593.7	585.8	586.8	581.9	569.1
Ref. [28]	587.5	578.3	572.3	566.8	551.2
Error (%)	1.06	1.30	2.53	2.66	3.25

Figure 4 illustrates the comparison between the numerical solution of the bilinear crack model and the open crack model. The results demonstrate consistency in the upper cycles, where the crack remains open. In contrast, during the lower cycles, the closing of the crack results in reduced equivalent stiffness, leading to discrepancies between the two models. In Figure 4a and 4c, the upper and lower peaks of the response for both the corresponding linear system (fully open crack model) and the final response obtained using the Runge-Kutta numerical method are presented. The results indicate that while the highest peaks of the two graphs coincide, discrepancies are observed in the lower peaks. These differences arise due to the closing of cracks during the lower peaks, which reduces the system's equivalent stiffness. To address this discrepancy, a first-order correction term is introduced, as illustrated in Figure 4b. It is noteworthy that in the upper peaks, where the two graphs overlap, the correction term approaches zero. Figure 5 compares the analytical solution derived using the Lindest-Poincaré perturbation method with the numerical solution for the bilinear crack model. The close alignment between the two responses validates the accuracy of the analytical method in capturing the nonlinear dynamics of the cracked beam.

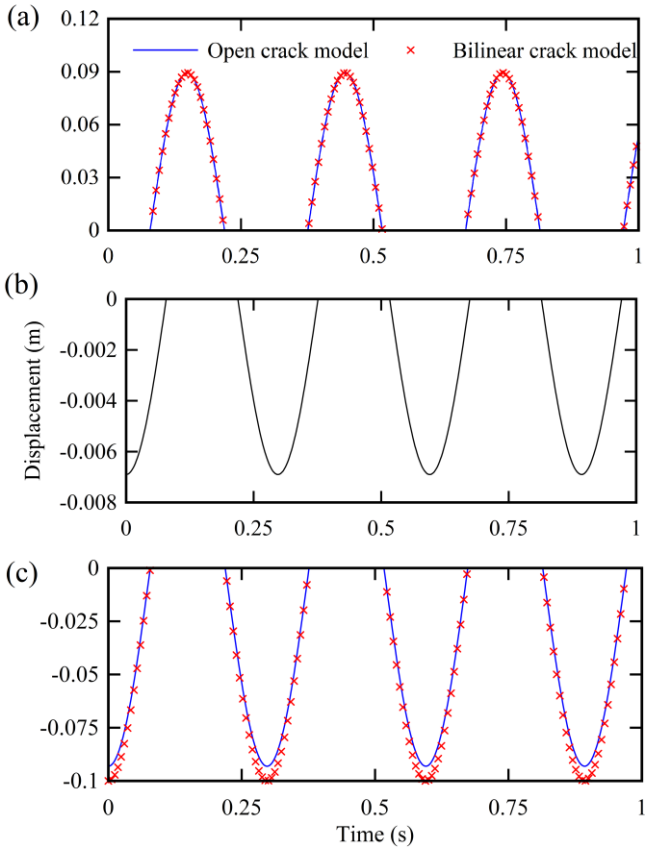

Fig. 4 - (a) Upper peaks of the response from the corresponding linear system (b) First-order correction term and (c) Lower peaks of the response from the corresponding linear system compared with the response obtained via the Runge-Kutta numerical method, for $\alpha = 0.4$ and $\beta = 0.4$.

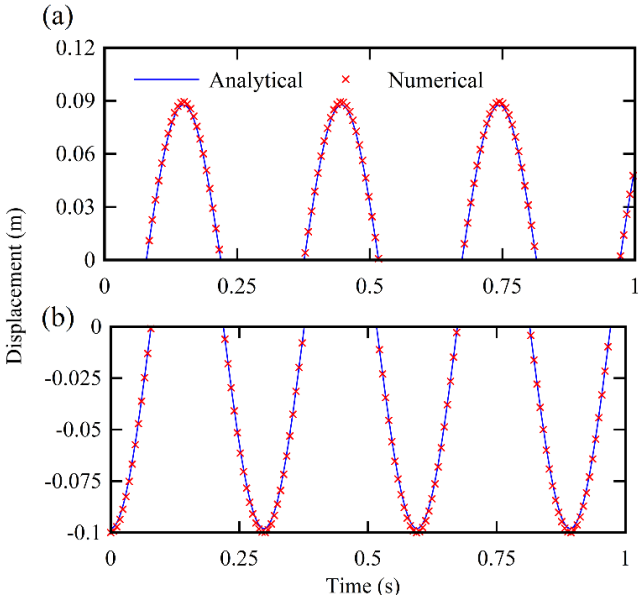

Fig. 5 - (a) Upper peaks and (b) Lower peaks of the response obtained via the Lindest-Poincaré method following the application of the first-order correction, alongside the response from the Runge-Kutta numerical method, for $\alpha = 0.4$and $\beta = 0.4$.

As the relative depth of a crack at a fixed position increases, its effect on the system's dynamic response is analyzed and presented in Figure 6. The results indicate a clear trend: the degree of reduction in the system's equivalent stiffness grows proportionally with the increase in crack depth. This reduction in stiffness introduces significant nonlinearities into the system's behavior, which, in turn, exacerbates the disparity between the response predicted by the numerical method and that of the corresponding linear system. A closer examination reveals that these discrepancies become particularly evident during the lower half-cycles of the system vibration. In this phase, the crack undergoes opening dynamics, resulting in a notable drop in the equivalent stiffness of the system. Consequently, the system exhibits larger deviations in the lower peaks of its response, as shown in Fig. 6. The lower peaks of the two graphs—representing the numerical method's reaction and the linear system's response—clearly illustrate this divergence. Furthermore, the increased crack depth not only magnifies the stiffness reduction but also intensifies the nonlinearity in the system's vibration behavior. This behavior underscores the critical role of crack parameters, such as depth, in influencing the system's dynamic characteristics. By comparing the lower peaks in Fig. 6, it becomes evident that the numerical method accurately captures the effects of crack dynamics, including the substantial impact of the crack opening and closing on the equivalent stiffness. These findings highlight the limitations of the linear system model in addressing such nonlinear effects and reinforce the necessity of incorporating nonlinear modeling approaches to achieve accurate predictions of the system's behavior under varying crack conditions.

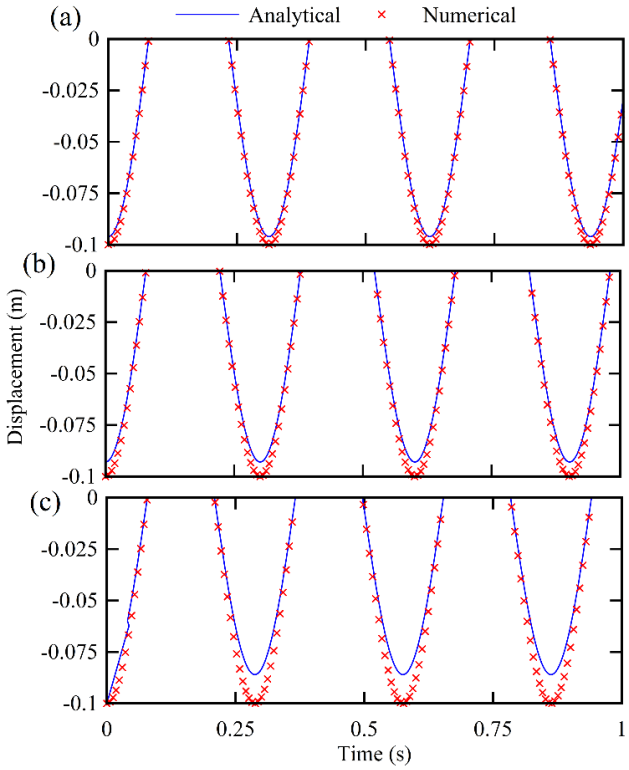

Fig. 6 - Comparison of the lower peaks of the response of the corresponding linear system and the final response obtained by the Rang-Kuta numerical method, for $\beta = 0.4$and relative depths of the crack (a) $\alpha = 0.2$, (b) $\alpha = 0.4$, and (c) $\alpha = 0.6$.

As the relative crack depth increases while maintaining a fixed relative position, a noticeable augmentation in the discrepancies between the response of the corresponding linear system and that acquired through numerical methods occurs. This discrepancy expansion consequently leads to an increase in the range of fluctuations observed in the first-order correction term. This noteworthy phenomenon is vividly depicted in Figure 7.

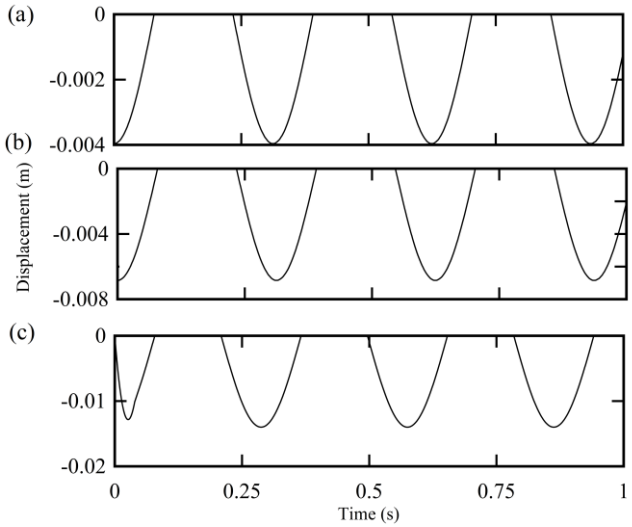

Fig. 7 - First-order correction term of the response obtained using the Lindest-Poincaré method for varying relative positions $\beta = 0.4$ and depths of the crack (a) $\alpha = 0.2$, (b) $\alpha = 0.4$, and (c) $\alpha = 0.6$.

The relative position of the crack, akin to the relative depth, exerts a notable effect on the vibration response of the cracked structure. In Figure 8, the impact of altering the crack's relative position while maintaining a constant relative depth on the range of fluctuations in the first-order correction term is explored. The first-order correction term's amplitude of fluctuations increases as the crack's location gets closer to the beam's cantilever end. This escalation signifies an intensified effect of crack opening and closing on the system's vibration response, consequently accentuating the system's nonlinear behavior. It is evident that the response of the system, with the application of the first-order correction, closely mirrors the final response obtained through numerical methods. The impact of the second-order correction term on the response is substantially lesser than that of the first-order correction term. However, it remains sensitive to crack parameters, exhibiting alterations in its shape during open and closed half-cycles.

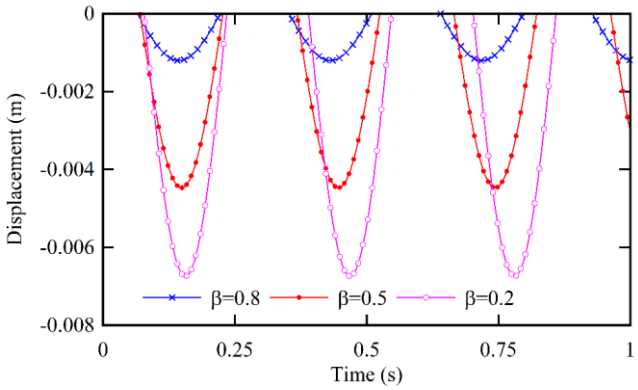

Fig. 8 - Correction term of the response obtained using the Lindest-Poincaré method for varying relative crack depths of $\alpha = 0.5$and positions (a) $\beta = 0.2$, (b) $\beta = 0.5$, and (c) $\beta = 0.8$.

Figure 9 illustrates the effect of increasing the relative depth of the crack while maintaining a fixed relative position, on the amplitude of fluctuations in the second-order correction term. The second-order correction term's range of variations grows in tandem with an increase in the relative fracture depth.

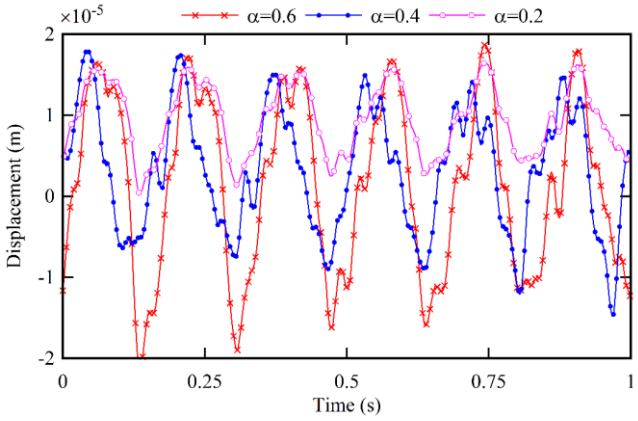

Fig. 9 - Second-order correction term of the response obtained using the Lindest-Poincaré method for relative positions $\beta = 0.4$ and for $\alpha = 0.2$, $\alpha = 0.4$ and $\alpha = 0.6$.

Furthermore, Figure 10 demonstrates how changes in the relative crack position affect the amplitude of fluctuations in the second-order correction term. As the crack's position approaches the end of the gripper with a fixed relative depth, the amplitude of fluctuations in the second-order correction term increases.

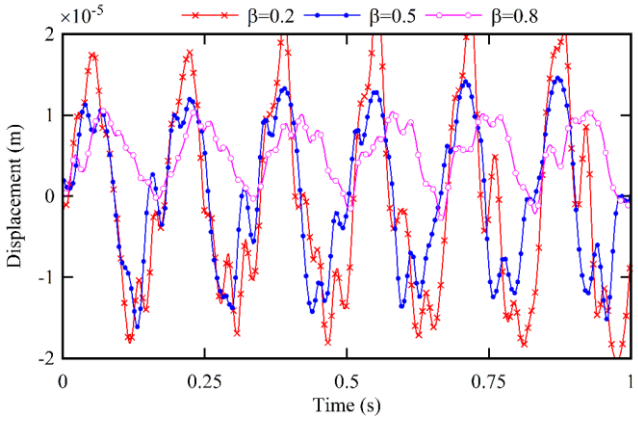

Fig. 10 - Second-order correction term of the response obtained using the perturbation method for relative crack depths of$\alpha = 0.5$and for $\beta = 0.2$, $\beta = 0.5$, and $\beta = 0.8$.

One of the primary features of the nonlinear behavior exhibited by the vibration response of a cracked structure, whether it possesses an open or closed crack, is the emergence of harmonic components in its response. In fact, the correction part of the answer obtained by the Lindest-Poincaré method, which is added to the first term of the answer in order to apply the crack opening and closing effects is presented in Eqs. (31) and (39), include harmonic components. Is. In Figure 11, the frequency response diagram obtained using the fast Fourier transform of the time trace obtained by the method presented in this research after adding the first-order correction term to the response of the corresponding linear system for the relative crack depth of $\alpha = 0.5$ and relative crack position of $\beta = 0.2$ is drawn. It is clear that the first-order correction term includes harmonics in even multiples of the system's natural frequency, in which the harmonic component of 2X has the greatest effect on the system's response. Figure 12 shows the frequency spectrum of the response after adding the first and second-order correction sentences to the response of the corresponding linear system in the case of relative crack depth of $\alpha = 0.5$ and relative crack position of=β 0.2 It becomes evident that upon incorporating the second-order correction term into the system response, odd-order harmonics emerge in the frequency spectrum of the response. This divergence arises from the fact that while the first-order correction term solely encompasses harmonic components in even

multiples of the system's natural frequency, the second-order correction term encompasses harmonic components in all integer multiples of the system's natural frequency. Given that even harmonics correspond to order (*2n*) and odd harmonics correspond to order (2*n*+1), the range of even harmonics notably surpasses that of odd harmonics. Experimental and analytical findings from reference [29] also corroborate this observation.

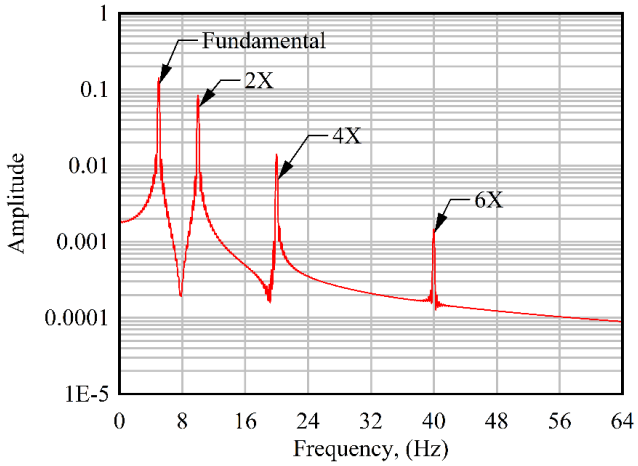

Fig. 11 - The frequency spectrum of the response, after the first-order correction term is applied, to changes in the relative location and depth of the fracture

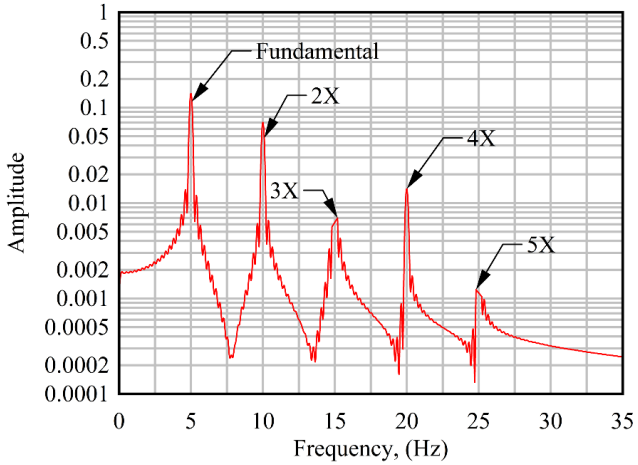

Fig. 12 - When the relative depth and relative location of the crack are disturbed, the frequency spectrum of the reaction following the application of the first and second-order corrective phrases

Figure 13 illustrates the variation in the natural frequency of the system under 2 conditions: assuming an open crack and assuming both open and closing crack states, as a function of the relative depth of the crack at a relatively fixed position. It is apparent that in both scenarios—assuming an open crack and assuming both open and closing crack states—the increase in crack parameters results in a reduction in natural frequencies. However, the decrease in natural frequencies when assuming both open and closing crack states is less pronounced than when assuming the crack is solely open.

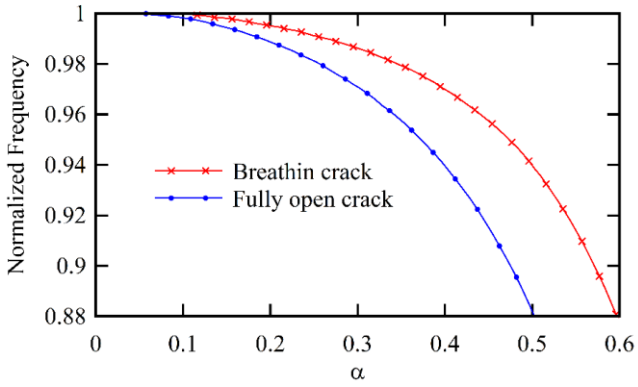

Fig. 13 - Dependent on the relative depth of the fracture in $\beta = 0.1$, variation in the natural frequency with the assumptions of a fully open crack and an open and closing crack

CONCLUSIONS

This study looked at the nonlinear behavior of free vibrations in a single-span beam with a transverse fatigue fracture. There was a proposal for a new model for the bilinear stiffness of the beam with a fatigue fracture. Using this model, the bilinear differential equation governing the behavior of the cracked beam was derived in an analyzable form through the Lindest-Poincaré method.

These findings reveal that the response obtained through the Lindest-Poincaré method comprises the aggregate response of the corresponding linear system and a series of correction terms. These correction terms account for the variations in the equivalent stiffness of the system during vibration induced by crack opening and closing, thereby incorporating harmonic components with correct coefficients of the system's natural frequency. This analysis elucidates the relationship between the nonlinear characteristics of the beam's behavior with fatigue cracks, as well as the harmonic components in the response, with the crack parameters and system characteristics. Notably, the correction terms encapsulate harmonic components in the response, with the governing rules expressing the analytical relationship between these components and the crack parameters and system characteristics. Furthermore, it is observed that the first-order correction term, which includes harmonic components in even multiples of the system's natural frequency, exerts a greater influence on the response compared to higher-order correction terms.

Comparison between the behavior derived from this analytical solution and numerical solutions demonstrates a high degree of concordance across a broad spectrum of crack parameters. Additionally, graphs depicting frequency changes with crack parameters in both the open and closed crack models utilized in this research highlight a lesser reduction in natural frequency caused by real fatigue cracks exhibiting open and closed behavior compared to cracks solely in an open state. This observation is further corroborated by experimental results reported in the technical literature.

REFERENCES

[1] Lee, Y.F. and Y. Lu (2022) Identification of fatigue crack under vibration by nonlinear guided waves. *Mechanical Systems and Signal Processing*, 163, 108138.
[2] Haiyan, Z., L. Shengrong, J. Mingze, W. Yi, S. Yang, L. Qiaodan, T. Zeyu, and X. Qian (2023) Review of research on the influence of vibration and thermal fatigue crack of brake disc on rail vehicles. *Engineering Failure Analysis*, 107603.
[3] Li, L., Z. Zhang, P. Zhang, and Z. Zhang (2023) A review on the fatigue cracking of twin boundaries: Crystallographic orientation and stacking fault energy. *Progress in Materials Science*, 131, 101011.
[4] Rezaee, M., H. Javadian, and V.A. Maleki (2015) Vibration behavior and crack detection of a cracked short beam under a axial load. *Mechanical Engineering*, 47(2).
[5] Eslami, G., V.A. Maleki, and M. Rezaee (2016) Effect of open crack on vibration behavior of a fluid-conveying pipe embedded in a visco-elastic medium. *Latin American Journal of Solids and Structures*, 13, 136-154.
[6] Xu, W., Z. Su, M. Radzieński, M. Cao, and W. Ostachowicz (2021) Nonlinear pseudo-force in a breathing crack to generate harmonics. *Journal of Sound and Vibration*, 492, 115734.
[7] Kushwaha, N. and V. Patel (2020) Modelling and analysis of a cracked rotor: a review of the literature and its implications. *Archive of Applied Mechanics*, 90(6), 1215-1245.
[8] Khosravi, S., S. Amirsardari, and M.A. Goudarzi (2024) Dynamic Behavior of Rectangular Tanks with Limited Freeboard Under Seismic Loads: Experimental, Analytical and Machine Learning Investigations. *Journal of Pressure Vessel Technology*, 1-34.
[9] Khosravi, S. and M.A. Goudarzi (2023) Seismic risk assessment of on-ground concrete cylindrical water tanks. *Innovative Infrastructure Solutions*, 8(1), 68.
[10] Khosravi, S., M.M. Yousefi, and M. Goudarzi (2021) Development of seismic fragility curves of cylindrical concrete tanks using nonlinear analysis. *Amirkabir Journal of Civil Engineering*, 53(1), 71-88.
[11] Spagnol, J., H. Wu, and C. Yang (2020) Application of non-symmetric bending principles on modelling fatigue crack behaviour and vibration of a cracked rotor. *Applied Sciences*, 10(2), 717.
[12] Wang, T., M. Noori, and W.A. Altabey (2021) Identification of cracks in an Euler–Bernoulli beam using Bayesian inference and closed-form solution of vibration modes. *Proceedings of the Institution of Mechanical Engineers, Part L: Journal of Materials: Design and Applications*, 235(2), 421-438.
[13] Li, H., T. Wang, and G. Wu (2023) Nonlinear vibration analysis of beam-like bridges with multiple breathing cracks under moving vehicle load. *Mechanical Systems and Signal Processing*, 186, 109866.
[14] Rezaee, M. and V. Maleki (2011) A New Nonlinear Model for Flexural Vibration Analysis of a Cracked Beam with a Fatigue Crack. *Journal of Applied and Computational Sciences in Mechanics*, 22(2), 35-52.
[15] Peng, Z., Z. Lang, and S. Billings (2007) Crack detection using nonlinear output frequency response functions. *Journal of Sound and Vibration*, 301(3-5), 777-788.
[16] Kharazan, M., S. Irani, M.A. Noorian, and M.R. Salimi (2021) Nonlinear vibration analysis of a cantilever beam with multiple breathing edge cracks. *International Journal of Non-Linear Mechanics*, 136, 103774.
[17] Dezfuli, M.A., M. Zeinoddini, and R.M. Harati (2020) An analytical model for the coupled-field dynamic fatigue crack growth in a metallic beam under chaotic excitations. *Theoretical and Applied Fracture Mechanics*, 109, 102726.
[18] Zhao, X., S. Li, W. Zhu, and Y. Li (2022) Nonlinear forced vibration analysis of a multi-cracked Euler-Bernoulli curved beam with inclusion of damping. *Mechanical Systems and Signal Processing*, 180, 109147.
[19] Ghaderi, M., H. Ghaffarzadeh, and V.A. Maleki (2015) Investigation of vibration and stability of cracked columns under axial load. *Earthquakes and Structures*, 9(6), 1181-1192.
[20] Long, H., Y. Liu, and K. Liu (2023) Vibration analysis of a cracked beam using the finite element method. *Transactions of the Canadian Society for Mechanical Engineering*.
[21] Aggumus, H., M. Daskin, M. Haskul, and A. Turan (2024) The Effect of the Crack-Stiffness Relationship on the System Response in Columns of an SDOF Steel Structure Model under Harmonic and Earthquake Excitations. *Shock and Vibration*, 2024(1), 9278849.
[22] Hai, T.T. and D. Nam (2023) A single degree of freedom model for cracked beam. *Vietnam Journal of Mechanics*, 45(2), 183-196.
[23] Liu, Y., W. Long, Y. Chen, and H. Hu (2024) Nonlinear vibration characteristics and damage detection method of blade with breathing fatigue crack. *Aerospace Science and Technology*, 155, 109715.
[24] Alshammrei, S., B. Lin, and J. Tong (2020) Full-field experimental and numerical characterisation of a growing fatigue crack in a stainless steel. *International Journal of Fatigue*, 133, 105449.
[25] Mukhopadhyay, M., *Structural Dynamics*. 2021: Springer.

[26] Dimarogonas, A.D., S.A. Paipetis, and T.G. Chondros, *Analytical methods in rotor dynamics*. 2013: Springer Science & Business Media.
[27] Nayfeh, A.H. and D.T. Mook, *Nonlinear oscillations*. 2008: John Wiley & Sons.
[28] Orhan, S. (2007) Analysis of free and forced vibration of a cracked cantilever beam. *Ndt & E International*, 40(6), 443-450.
[29] Saavedra, P. and L. Cuitino (2001) Crack detection and vibration behavior of cracked beams. *Computers & Structures*, 79(16), 1451-1459.